

Influence of magnetic interaction between impurity and impurity-liberated spins on the magnetism in the doped Haldane chain compounds $\text{PbNi}_{2-x}\text{A}_x\text{V}_2\text{O}_8$ ($\text{A} = \text{Mg}, \text{Co}$)

Andrej Zorko* and Denis Arčon

Jožef Stefan Institute, Jamova 39, 1000 Ljubljana, Slovenia

Alexandros Lappas

Institute of Electronic Structure and Laser, Foundation for Research and Technology - Hellas, P.O. Box 1527, 71110 Heraklion, Crete, Greece

Zvonko Jagličić

Institute of Mathematics, Physics and Mechanics, Jadranska 19, 1000 Ljubljana, Slovenia

(Dated: December 7, 2018)

A comprehensive study of impurity-induced magnetism in nonmagnetically (Mg^{2+}) and magnetically (Co^{2+}) doped $\text{PbNi}_2\text{V}_2\text{O}_8$ compounds is given, using both macroscopic dc susceptibility and local-probe electron spin resonance (ESR) techniques. Magnetic coupling between impurity-liberated spins is estimated from a linewidth of low-temperature ESR signal in Mg-doped samples. In addition, in the case of magnetic cobalt dopants the impurity-host magnetic exchange is evaluated from the Co-induced contribution to the linewidth in the paramagnetic phase. The experimentally observed severe broadening of the ESR lines in the magnetically doped compounds with respect to nonmagnetic doping is attributed to a rapid spin-lattice relaxation of the Co^{2+} ions, which results in a bottleneck-type of temperature dependence of the induced linewidth. The exchange parameters obtained from the ESR analysis offer a satisfactory explanation of the observed low-temperature magnetization in doped samples.

PACS numbers: 75.50.Mm, 75.30.Hx, 76.30.Fc

I. INTRODUCTION

Haldane integer-spin chains with antiferromagnetic coupling have been extensively studied experimentally as well as theoretically in the last two decades. This is due to their fascinating property conjectured by Haldane [1]. Namely, in contrast to half-integer-spin chains, in integer-spin chains a quantum disordered singlet ground state with correlations decaying exponentially is separated from the lowest excited state (spin gap). Such character of the Haldane chains with only the nearest-neighbor (nn) isotropic antiferromagnetic exchange coupling was satisfactorily accounted for by the valence-bond-solid model [2], which introduced valence bonds emerging and terminating at neighboring sites. The validity of this model was experimentally confirmed for the first time in the spin $S = 1$ compound NENP by observing $S = 1/2$ liberated end-chain spins when a portion of the valence bonds was intentionally broken by introducing impurities to partially replace the $S = 1$ spins [3].

In general, impurities have been in the past often deliberately introduced to host materials and thus employed to reveal the magnetic character of the host. The instructive examples cover a variety of different low-dimensional quantum spin systems including high- T_c superconductors [4]. Moreover, the impurities can dramatically affect the ground state of the host material leading to unex-

pected magnetic phenomena. One of their most astonishing consequences is the induction of long-range magnetic ordering upon doping, an effect known as “order-by-disorder effect” [5], where disorder in a form of random doping causes magnetic ordering in the host material. This mechanism is known to set-in in different spin-gap systems including the spin-Peierls compound CuGeO_3 substitutionally doped with different nonmagnetic [6, 7, 8] or magnetic ions [7, 9], the vacancy doped two-leg spin-ladder compound SrCuO_3 [10] and the three-dimensional coupled-spin-dimer system TlCuCl_3 doped with nonmagnetic impurities [11]. Recently, also the first Haldane-chain compound $\text{PbNi}_2\text{V}_2\text{O}_8$ that undergoes a transition to a magnetically ordered ground state at low temperatures when doped with either nonmagnetic [12] Mg^{2+} or magnetic [13, 14] Co^{2+} , Cu^{2+} and Mn^{2+} ions on Ni^{2+} ($S = 1$) sites, was reported. There are several common features of the phase transitions in the above-mentioned systems, the first one being that already a very small amount of impurities induces long-range ordering. Second, it appears universal that the phase-transition temperature increases as a function of the doping level at low concentrations and decreases at higher concentrations [8, 10, 11, 14, 15]. Therefore, a quest to find a unified picture, which would satisfactorily explain the impurity-induced long-range ordering in spin-gap systems, is currently underway.

The way to magnetic ordering in the spin-gap systems is paved by clusters of exponentially decaying staggered moments induced next to the impurity sites [16], which are magnetically coupled through the gaped medium.

*Electronic address: andrej.zorko@ijs.si

Weak coupling results in in-gap energy states, which dominate the low-temperature magnetic character of the doped systems. However, the picture of the impurity-induced magnetic ordering in spin-gap systems still remains rather unclear. In particular, the mechanisms leading to the development of three-dimensional intercluster spin correlations are particularly elusive. In order to elucidate this intriguing phenomenon it is crucial to develop a deeper understanding of the magnetic interactions within the pockets of the impurity-induced staggered moments as well as between them.

Therefore, we decided to act upon a comprehensive magnetic investigation of the Haldane chain compound $\text{PbNi}_2\text{V}_2\text{O}_8$ doped with nonmagnetic Mg^{2+} and magnetic Co^{2+} impurities. The study incorporates macroscopic dc susceptibility measurements and local-scale magnetic resonance techniques, which already proved to yield invaluable information on the impurity-induced magnetism in Mg-doped compounds [17, 18]. The results of the electron spin resonance (ESR) are displayed in the present paper while the findings of the complementary nuclear magnetic resonance (NMR) measurements on ^{51}V nuclei weakly coupled to electronic moments, are presented elsewhere [19]. Combining the results of the dc susceptibility measurements and the ESR technique, we are able to evaluate the magnetic coupling within the impurity-induced pockets of staggered moments as well as to highlight the role of the intercluster coupling on the long-range magnetic ordering.

II. EXPERIMENTAL DETAILS

Polycrystalline samples were prepared by a solid-state reaction with the details of the procedure already been published [20]. The efficiency of the Mg^{2+} and Co^{2+} cations replacements for Ni^{2+} ions was experimentally verified by powder x-ray and neutron diffraction [21, 22]. The presence of any impurity phases was limited below the sensitivity level of the x-ray diffractometer. dc magnetization measurements were performed on a Quantum Design SQUID magnetometer in a magnetic field of 100 mT down to 2 K. For ESR measurement a Bruker E580 FT/CW spectrometer was used. These measurements were conducted between room temperature and 5 K at a Larmor frequency of $\nu_L \approx 9.4$ GHz (X-band).

III. EXPERIMENTAL RESULTS

A. dc susceptibility

As previously reported, doping the $\text{PbNi}_2\text{V}_2\text{O}_8$ compound with either nonmagnetic Mg^{2+} or magnetic Co^{2+} impurities results in the long-range magnetic ordering at low temperatures [12, 15]. Evidence to the nature of the ground state arise from the presence of sharp magnetic Bragg peaks in the neutron powder patterns

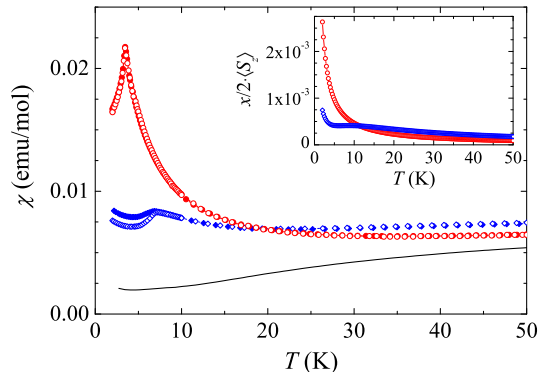


FIG. 1: (Color online) dc magnetic susceptibility of the $\text{PbNi}_{1.88}\text{Mg}_{0.12}\text{V}_2\text{O}_8$ (circles) and $\text{PbNi}_{1.92}\text{Co}_{0.08}\text{V}_2\text{O}_8$ (diamonds) compounds in the field cooling (solid symbols) and zero-field cooling (open symbols) regime in the magnetic field of 100 mT. The solid line is displaying the spin-gap behavior of the pristine $\text{PbNi}_2\text{V}_2\text{O}_8$ material. Inset shows a temperature evolution of the average impurity-induced spin size for $S = 0$ (circles) and $S = 3/2$ (diamonds) impurities in a simplified model described in subsection IV C.

[20, 22]. The onset of the magnetic ordering is clearly expressed in the characteristic peaks of the magnetic susceptibility curves at low temperatures as shown in Fig. 1. The transition temperatures in the external magnetic field of 100 mT are around 3.4 K and 7.1 K in the case of $\text{PbNi}_{1.88}\text{Mg}_{0.12}\text{V}_2\text{O}_8$ and $\text{PbNi}_{1.92}\text{Co}_{0.08}\text{V}_2\text{O}_8$, respectively.

The first rather unusual feature of the observed phase transition is the significantly different value of the phase-transition temperature in both materials, although the stoichiometric amounts of impurities are similar. Such an increase of the transition temperature in the case of cobalt doping compared to nonmagnetic doping was not observed in the immensely studied CuGeO_3 compound, which is a prototypical system for impurity-induced magnetic ordering [6, 7, 8, 9]. However, it is in line with the observation that the magnetically ordered state is much more stable against the external magnetic field in Co-doped $\text{PbNi}_2\text{V}_2\text{O}_8$ than in Mg-doped samples, as experimentally verified by dc magnetization and NMR measurement in magnetic fields of several Tesla [19]

Apart from the significant increase of the transition temperature in the Co-doped compound, another feature is noticeable in Fig. 1. Namely, while the Mg-doped sample exhibits no hysteresis between the zero-field cooling (ZFC) and field cooling (FC) regimes in the magnetically ordered state, such behavior is observed in the case of the Co-doped sample. This experimental finding seems unusual in the light of the neutron diffraction performed on both compounds in the magnetically ordered state, suggesting a magnetic ordering of similar character. More specifically, purely magnetic neutron diffraction patterns indicate that the average magnetic moment per Ni site pointing along the direction of the Ni chains (c axis) is in

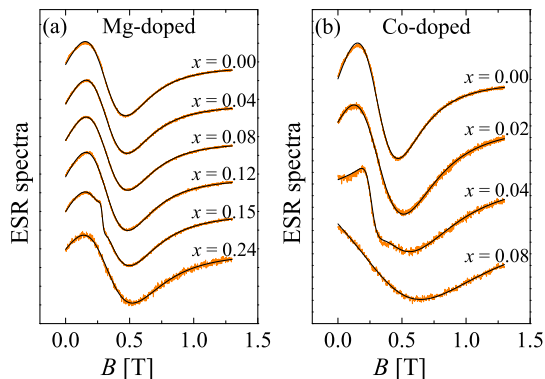


FIG. 2: (Color online) The evolution of the room-temperature X-band ESR spectra of $\text{PbNi}_{2-x}\text{A}_x\text{V}_2\text{O}_8$ with increased level of doping in the case of (a) nonmagnetic $\text{A} = \text{Mg}^{2+}$ and (b) magnetic $\text{A} = \text{Co}^{2+}$ dopants. The solid lines represent fits to broad Lorentzian distribution as explained in the text.

both compounds close to $1\mu_B$ [21, 22]. These measurements, however, can not yield information on the components of the magnetic moments perpendicular to the chains due to the uniaxial symmetry of the lattice and the powder nature of the samples. It has been recently argued by Imai et al. [14] that the observed irreversibility between the ZFC and FC measurements is not a signature of a spin-glass behavior but should rather be due to the occurrence of weak ferromagnetism in Co-doped samples, attributed to the presence of the Dzyaloshinsky-Moriya (DM) interaction [23, 24]. Such antisymmetric anisotropic interaction is indeed present between Ni spins [25], however, the general anisotropic exchange between impurity and host spins should be involved in the ZFC/FC irreversibility.

Although the nominal concentrations of impurities in both samples are similar, the low-temperature peak in the magnetic susceptibility is much more pronounced in the Mg-doped sample despite the fact that Mg dopants are nonmagnetic. The uniform static spin susceptibility can be obtained from the dynamical spin structure factor $S^{zz}(\mathbf{q}, \omega) = \text{Re} \int_0^\infty e^{i\omega t} \langle S_{\mathbf{q}}^z(t) S_{-\mathbf{q}}^z(0) \rangle dt$, reflecting the distribution of the spectral weight of spin excitations (the brackets (...) denote statistical averaging). Kramers-Kronig relations give the following expression

$$\chi_0 \propto \frac{1}{\pi} \lim_{\mathbf{q} \rightarrow 0} \mathcal{P} \int_{-\infty}^{\infty} \left(1 - e^{-\hbar\omega/k_B T}\right) \frac{S^{zz}(\mathbf{q}, \omega)}{\omega} d\omega, \quad (1)$$

where \mathcal{P} stands for the Cauchy principle value. Bering in mind that the static susceptibility is dominated by low-energy spin excitations, the intensities of the low-temperature magnetic susceptibility give a clear signal that the in-gap impurity-induced density of states is peaked at much lower frequencies when magnesium impurities are present. This is not surprising, as stronger

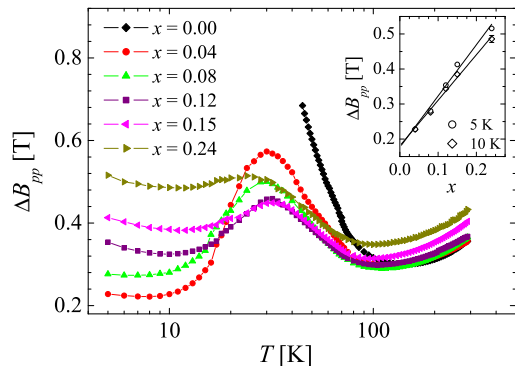


FIG. 3: (Color online) The temperature dependence of the X-band ESR linewidth in $\text{PbNi}_{2-x}\text{Mg}_x\text{V}_2\text{O}_8$ compounds. Inset shown a linear dependence of the impurity-induced line broadening at 5 K and 10 K.

magnetic coupling is expected in the case of cobalt impurities, which shifts the in-gap states to higher energies. Moreover, our analysis based on the parameters obtained from the ESR results, gives also a quantitative agreement, as demonstrated in the subsection IV C.

B. Electron spin resonance

As previously reported, X-band ESR absorption spectra of the $\text{PbNi}_2\text{V}_2\text{O}_8$ are fairly broad at room temperature and further broaden with lowering the temperature [17]. Partial substitution of the magnetic Ni^{2+} ions with nonmagnetic Mg^{2+} ions results in additional broadening of the resonance lines, which moderately increases with the level of doping as clearly observed in Fig. 2a. On the other hand, the case of Co-doping results in extreme broadening of the ESR spectra (Fig. 2b), reflecting the magnetic nature of the dopants.

All the spectra can be satisfactory fitted with a broad Lorentzian function taking into account the resonant absorption at positive as well as negative resonant field. In addition, some samples require an extra narrow component, whose intensity proves to be sample dependent even within the same nominal stoichiometry. This fact allows us to attribute this additional signal to impurity phases present in the sample. However, judged from very small relative intensities of the spurious signals (i.e., below 1%) such impurities would be unobservable in x-ray diffraction patterns.

With lowering temperature a diverse nature of the ESR spectra in Mg-doped samples becomes evident (see Fig. 3). Based on the scaling of the low-temperature ESR intensities with the doping level and the temperature evolution of the observed g -factor shifts [17], we were previously able to attribute the additional low-temperature signal in vacancy-doped samples to impurity-liberated end-chain degrees of freedom, which are delocalized on

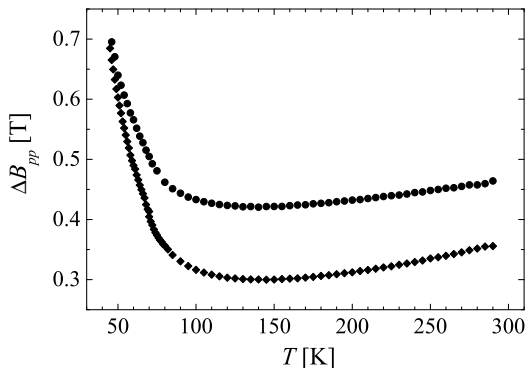


FIG. 4: The temperature dependence of the ESR linewidth in $\text{PbNi}_{1.98}\text{Co}_{0.02}\text{V}_2\text{O}_8$ (circles) compared to $\text{PbNi}_2\text{V}_2\text{O}_8$ (diamonds).

the scale of the correlation length ξ [26]. It was further argued that these end-chain spins at both sides of a particular impurity were ferromagnetically coupled through interchain exchange providing a mechanism for three-dimensional magnetic ordering. Such ferromagnetic coupling was indeed later experimentally confirmed by specific heat measurements reported by Masuda et al. [27]. The exact origin of the rather broad low-temperature ESR signals still, however, remains to be revealed. The ESR linewidth reflects the strength of the magnetic coupling between liberated spins, which makes its analysis invaluable for the understanding of the impurity-induced magnetism.

In Co-doped samples we were able to follow the temperature evolution of the spectra below room temperature only in the case of the sample with the lowest doping level, i.e., in $\text{PbNi}_{1.98}\text{Co}_{0.02}\text{V}_2\text{O}_8$. The ESR linewidth of this compound is compared to the linewidth of the pristine compound in Fig. 4. It exhibits a rather different behavior from the case of the Mg-doped materials as the linewidths of the two samples are clearly converging towards the same values when decreasing the temperature. To explain the extreme broadening of the ESR spectra due to Co^{2+} ions and a bottleneck-type of the impurity-induced contribution to the ESR linewidth, the spin nature of the dopants is successfully incorporated into the analysis in the next section.

IV. ANALYSIS AND DISCUSSION

A. ESR measurements in the paramagnetic phase

To rationalize the observed broadening of the ESR spectra at room temperature due to doping (Fig. 2), we presume that the impurities do not have any noticeable effect on the crystal structure of the materials [21, 22]. Since the dominant spin anisotropy contributions in the investigated materials are of single-ion anisotropy type

[28] and DM type [25], it can be assumed that they do not change appreciably at Ni sites when dopants are introduced. Therefore, the impurities have to influence the time-evolution of spin correlation functions entering the expression of the ESR linewidth. The peak-to-peak linewidth of the Lorentzian line in the exchange-narrowing limit is given by [29]

$$\Delta B_{pp} = \frac{C}{g\mu_B} \left(\frac{M_2^3}{M_4} \right)^{1/2}. \quad (2)$$

Here C denotes a constant of the order of unity and g the g -factor, while the second and the fourth moment of the absorption lines are given as

$$M_2 = \frac{\langle [\mathcal{H}', M^+] [M^-, \mathcal{H}'] \rangle}{\langle M^+ M^- \rangle}, \quad (3)$$

$$M_4 = \frac{\langle [\mathcal{H} - \mathcal{H}_Z, [\mathcal{H}', M^+]] [\mathcal{H} - \mathcal{H}_Z, [\mathcal{H}', M^-]] \rangle}{\langle M^+ M^- \rangle}. \quad (4)$$

The Hamiltonian $\mathcal{H} = \mathcal{H}_0 + \mathcal{H}'$ of the system is conventionally divided into two parts. The main part $\mathcal{H}_0 = \mathcal{H}_Z + \mathcal{H}_e$ contains only the Zeeman Hamiltonian \mathcal{H}_Z and the exchange Hamiltonian \mathcal{H}_e of the host. The perturbative part \mathcal{H}' includes all the anisotropy contributions of the host as well as the impurity Hamiltonian $\mathcal{H}^i = \mathcal{H}_Z^i + \mathcal{H}_e^{i-h} + \mathcal{H}_{LS}$ [30], where \mathcal{H}_Z^i denotes the Zeeman Hamiltonian of the impurity system, \mathcal{H}_{ex}^{i-h} the impurity-host exchange coupling and \mathcal{H}_{LS} the impurity spin-orbit coupling, all these terms being nonzero in the case of doping with magnetic dopants.

1. Mg-doping

In fact, the spin correlations can be significantly affected by impurities [31] in low-dimensional systems, where the exchange pathways are severely limited and the diffusional decay of spin correlations at longer times becomes important [32]. The rate of spin diffusion across the impurity site depends on the size of the impurity spin and the impurity-host exchange coupling [33]. Non-magnetic impurities act as reflecting agents, disabling the spin polarization to diffuse away and thus effectively diminishing the exchange-narrowing mechanism. A significant impurity-induced broadening of the ESR absorption lines is thus expected [32]. However, the observed broadening, presented in Fig. 5a, is not that prominent. This experimental finding can be explained by the relatively large interchain exchange coupling J_1 in the case of the $\text{PbNi}_2\text{V}_2\text{O}_8$ compound, $|zJ_1/J| \approx 0.03$, where $J = 95$ K (in units of k_B) represents the dominant nn intrachain exchange [28]. Hence the spin system behaves as three-dimensional on the X-band ESR time-scale since the out-of-chain diffusion rate, given by J_1/\hbar , is larger than the ESR frequency. The inhibited diffusion along the chains thus only partially influences the decay of spin correlations, which is also in line with the Lorentzian lineshape of the recorded ESR spectra [32].

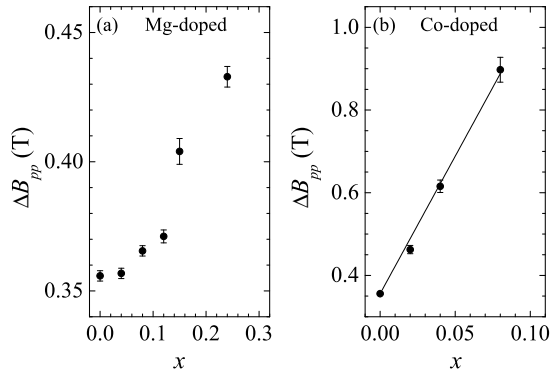


FIG. 5: Linewidth of the X-band ESR spectra recorded at room temperature in (a) Mg-doped and (b) Co-doped $\text{PbNi}_2\text{V}_2\text{O}_8$.

2. Co-doping

Significantly more pronounced is the broadening of the ESR spectra in the case of doping the parent $\text{PbNi}_2\text{V}_2\text{O}_8$ compound with magnetic Co^{2+} ions (see Fig. 5). We attribute the observed ESR signals solely to magnetic moments of the host (Ni^{2+}) spin system. Below-presented analysis shows that Co^{2+} magnetic moments are strongly affected by the spin-lattice relaxation at the room temperature, which severely broadens the ESR spectra.

When the Co^{2+} ion ($3d^7$ configuration) is placed into a crystal field, which arises from octahedrally coordinated O^{2-} ions, the ground orbital state is a triplet. Taking into account the spin $S = 3/2$ of the “high-spin” cobalt results in a twelve-fold degenerated ground state. The spin-orbit coupling and a distortion away from the cubic symmetry, as is the case in $\text{PbNi}_2\text{V}_2\text{O}_8$ [22], splits the energy levels, however, there remains a significant amount of orbital moment in the ground state [34]. The spin dynamics of Co^{2+} ions are strongly affected by lattice vibrations through the spin-orbit coupling. Extreme broadening of ESR lines due to a presence of small concentrations of Co^{2+} ions was reported in the past in several systems [30, 35, 36]. As Co^{2+} is a strongly relaxing ion, the broadening can be attributed to an interplay between impurity-host cross relaxation and spin-lattice relaxation of the impurity. The effect of the impurities is determined by the relative rate of the magnetic energy flow from the host to the impurity system with respect to the rate of the energy flow between the impurities and the underlying lattice. The expected ESR linewidth can then be expressed by the equation [35]

$$\Delta B_{pp} = \Delta B_0 + \frac{\eta}{1 + \eta} \Delta B_i, \quad (5)$$

where ΔB_0 represents the linewidth of the pristine compound, ΔB_i the impurity-induced contribution to the linewidth and $\eta = \omega_{sl}/\omega_e^{i-h}$ the ratio between the rate

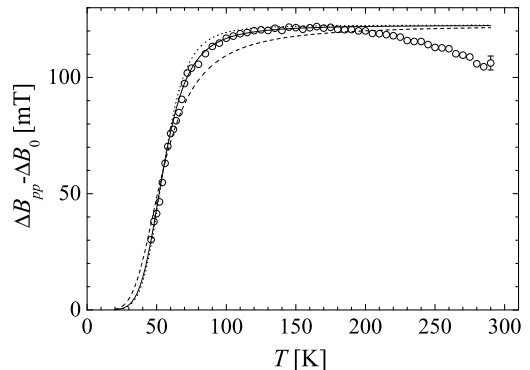


FIG. 6: The bottleneck behavior of the impurity-induced linewidth in $\text{PbNi}_{1.98}\text{Co}_{0.02}\text{V}_2\text{O}_8$. The curves represent the temperature dependence predicted by the model Eqs. (5)-(7) with the Debye temperature values $\theta_D = 300$ K (dashed line), $\theta_D = 500$ K (solid line) and $\theta_D = 700$ K (dotted line).

of the impurity spin-lattice relaxation and the impurity-host cross relaxation determined by the impurity-host exchange J_{i-h} . A bottleneck effect is expected to be observed since at low temperatures the spin-lattice relaxation of the impurity spins is far below the impurity-host cross relaxation.

As apparent from Fig. 6, the difference between the linewidth of the pure $\text{PbNi}_2\text{V}_2\text{O}_8$ and the $\text{PbNi}_{1.98}\text{Co}_{0.02}\text{V}_2\text{O}_8$ compounds indeed increases with temperature from 45 K, which represents the lowest temperature where the analysis is still reliable due to severe broadening at lower temperatures (see Fig. 4). The impurity-induced linewidth contribution reaches a broad maximum of approximately $\Delta B_i^{max} = 120$ mT around 150 K. The observed downturn at higher temperatures will be discussed in the end of this subsection. Such dependence is in line with the spin-lattice relaxation, which increases with temperature due to the temperature-activated phonon density. Spin-lattice relaxation of the impurities is expected to be due to Raman spin-phonon processes and can be written as [37]

$$\omega_{sl} = \frac{1}{T_1} = a \left(\frac{T}{\theta_D} \right)^\gamma \int_0^{\theta_D/T} \frac{y^6 e^y}{(e^y - 1)^2} dy. \quad (6)$$

In Eq. (6), parameter y is defined as $y = \hbar\omega/k_B T$, θ_D represents the Debye temperature and a is a constant depending on the strength of the spin-phonon coupling. The latter two constants are not known in our case, however, the a constant can be conveniently dismissed from the expression for the expected linewidth if we set $\eta(55 \text{ K}) = 1$ as the experimental impurity broadening reaches half of its saturated value at 55 K. In this case the parameter $\eta(T)$ can be expressed as

$$\eta(T) = \frac{\omega_{sl}(T)}{\omega_{sl}(55 \text{ K})}. \quad (7)$$

The fit of the model described through Eqs. (5)-(7) to the experimentally determined impurity-induced linewidth of the ESR spectra is satisfactory for temperatures below 200 K. The best agreement is reached when the Debye temperature is set to $\theta = 500$ K (solid line in Fig. 6). To see the effect of this parameter on the quality of the fit, theoretical curves with $\theta = 300$ K (dashed line) and $\theta = 700$ K (dotted line) are also shown in Fig. 6, which allows us to determine the Debye temperature of the $\text{PbNi}_2\text{V}_2\text{O}_8$ compound as $\theta = 500(50)$ K.

Furthermore, the saturated value of the impurity-induced linewidth contribution can be used for the estimation of the impurity-host exchange interaction. When the isotropic exchange coupling is the leading impurity-host interaction the following equation can be derived in the high-temperature limit [30]

$$\Delta B_i^{\max} = \frac{1}{\sqrt{3}} \frac{32}{g\mu_B} \frac{J_{i-h}^2 S_i(S_i+1)}{3\hbar\omega_e} \frac{x}{2}. \quad (8)$$

Here S_i denotes the size of the impurity spin, while the exchange frequency is defined as $\hbar\omega_e = \sqrt{M_4/M_2}$. In the case of the $\text{PbNi}_2\text{V}_2\text{O}_8$ compound the single-ion anisotropy of the form $D \cdot S_z^2$ was reported to be the leading anisotropy term, with $D = -5.2$ K determined from inelastic neutron scattering experiments [28]. The easy axis was found to point along the crystal c axis (direction of spin chains). Using Eqs. (3) and (4) one can then derive the following expressions for the exchange frequency $\omega_e = \sqrt{8}J/\hbar$, which predicts the impurity-host exchange of the size $J_{i-h} = 14$ K. The linear dependence of the induced line broadening as predicted by Eq. (8) is nicely revealed in Fig. 5b. The slope of this line (6.8 T) makes an estimation of the impurity-host exchange $J_{i-h} = 15$ K, which is only slightly different from the above value. Although the sign of J_{i-h} can not be determined from the above-presented ESR analysis, the magnetic susceptibility measurements speak in favour of antiferromagnetic coupling, as argued in subsection IV C.

The reduction of the Co-Ni exchange J_{i-h} with respect to the Ni-Ni intrachain exchange coupling J is expected. Namely, it is well established that the strength of the antiferromagnetic superexchange decreases with the reduction of the number of electrons in the $3d$ orbital. For instance, the Néel temperature of the NiO oxide with NaCl crystal structure reduces from 525 K to 290 K in CoO oxide [38]. Another example are the K_2AF_4 compounds (A is a transition metal ion), where the following exchange parameters were obtained: $J_{\text{Ni}} = 102$ K, $J_{\text{Co}} = 16.8$ K, $J_{\text{Fe}} = 15.7$ K, $J_{\text{Mn}} = 8.4$ K [36].

At the end of this subsection, a short explanation of the downturn of the impurity-induced linewidth above 150 K (see Fig. 6) is given. When the cobalt spin-lattice relaxation surpassed the above evaluated exchange frequency of the pure system, the spin fluctuations at nickel sites will become strongly affected by the spin-lattice relaxation due to the strong exchange coupling with cobalt ions [35]. For $\omega_{sl} \gg \omega_e$ the spin-lattice relaxation rate effectively substitutes the exchange frequency in Eq. (8)

[39], which results in a narrowing of the absorption lines with raising temperature due to the increase of the spin-lattice relaxation rate. Such narrowing was experimentally observed in KMnF_3 doped with Fe^{2+} ions [40]. If we approximate the rate of the impurity-host cross relaxation as $\omega_e^{i-h} \approx J_{i-h}/\hbar$ and take into account that $\omega_{sl}(55 \text{ K}) = \omega_e^{i-h}$, the Eq. (6) will allow us to make an estimation that $\omega_{sl} > \omega_e$ for $T > 100$ K. This corresponds fairly well with the temperature of 150 K where ΔB_i exhibits its maximum. The effect is, however, not as drastic as one might naively expect, which is due to the rather low concentration of Co^{2+} impurities.

B. ESR measurements within the Haldane-gap regime

At temperatures below the average Haldane gap $\Delta = 43$ K of the $\text{PbNi}_2\text{V}_2\text{O}_8$ system [28], in the Mg-doped compounds the tendency of line broadening with lowering temperature suddenly alters (see Fig. 3). In the mid-temperatures crossover regime, i.e., at $T \leq \Delta$, the single almost Lorentzian resonance line speaks in favour of a strong coupling of the liberated end-chain spins to the triplet Haldane excitations. Similarly to the NMR results on Mg-doped compounds [18] the one-dimensional Haldane excitations are thus again shown to coexist with the spin excitations emerging from the end-chain spins.

The low-temperature signal, i.e., below 10 K where Haldane excitations are severely suppressed due to the Haldane gap, can be exploited to obtain an insight into the nature of the magnetic interactions between the liberated spin degrees of freedom, which are responsible for the occurrence of the magnetic ordering. As already emphasized and again supported by the analysis presented in the subsequent subsection, the coupling of the two spins neighboring a particular vacancy site is ferromagnetic. Such ferromagnetic coupling effectively produced an anisotropy Hamiltonian of the single-ion form $D^* \tilde{S}_z^2$, where \tilde{S}_z represents an effective spin operator of the two-spin system. The size of the anisotropy in the case of the uniaxial symmetry is given by [41]

$$D^* = -\frac{3\mu_0}{4\pi} \frac{(g\mu_0)^2}{r^3} - \frac{3}{2} \left(\frac{\Delta g}{g} \right)^2 \tilde{J}'. \quad (9)$$

In Eq. (9) the first term arises from the dipolar coupling of the two spins and the second one represents the symmetric anisotropic exchange. The parameter \tilde{J}' stands for the effective ferromagnetic coupling between the two spins, which in our case is a result of the competing antiferromagnetic next-nearest neighbor exchange of the pure chain, $J' = 5$ K, and the ferromagnetic coupling mediated through neighboring chains [42]. In addition, the antisymmetric anisotropic exchange of the Dzyaloshinsky-Moriya type should also be included,

$$d \approx \left| (\Delta g/g) \tilde{J}' \right|. \quad (10)$$

From the known lattice parameters [22] the dipolar field at Ni^{2+} sites can be estimated, $B_{dd} = 45$ mT. This value is approximately twice larger than maximum internal fields observed in zero-field μ^+ -SR experiments [20]. The estimated value of the dipolar field is, however, far below the experimentally observed linewidths at low temperatures. This fact favours the DM interaction as the dominant broadening mechanism (first order in $\Delta g/g$).

A plot of the linewidth of the ESR spectra at 5 K and 10 K reveals a clear linear dependence upon the doping level (see inset of Fig. 3). Such linear dependence has been observed before in CuGeO_3 and attributed to the interacting delocalized spin clusters induced next to the impurities [43]. In the case of $\text{PbNi}_2\text{V}_2\text{O}_8$ the spin clusters exhibit an exponential decay of spin polarization with the correlation length $\xi \approx 6$ at $T = 0$ [26]. Apart from the interaction of the two clusters neighboring a particular spin vacancy and forming an effective spin $\tilde{S} = 1$, there is thus an additional sizable anisotropic interaction between neighboring $\tilde{S} = 1$ effective spins on the chain, which increases with the level of doping as reflected in the increase of the linewidth.

The zero-doping values of the linewidth can be assigned to be due to the intrinsic anisotropy of the uncoupled effective $\tilde{S} = 1$ impurity-induced spins. These values are virtually the same at 5 K and 10 K, i.e., $\Delta B_{pp}^{x=0} = 180$ mT, which is in favour of the above assumption. Namely, due to the gapped nature of magnetic excitations of the mediating Haldane medium, the effective $\tilde{S} = 1$ spins can be regarded as isolated in the limit $x \rightarrow 0$. The increase of the linewidth below 10 K, which can be either due to the critical enhancement of antiferromagnetic correlations close to the phase transition temperature [17] or a signature of the temperature evolution of the correlation length [26], consequently does not affect the zero-doping linewidth. This value can then be used for an estimation of the effective ferromagnetic coupling within the effective $\tilde{S} = 1$ spins, which is according to Eq. (10) of the size $\tilde{J}' = -2$ K. In this estimation the room-temperature value of $\Delta g/g = 0.1$, which is not affected by static spin correlations, was taken into account, as well as the fact that the exchange narrowing mechanism is not active in diluted magnetic systems [37].

C. Susceptibility of the impurity induced in-gap states

Using the above results of the exchange coupling between the impurity-induced spins \tilde{J}' and impurity-host coupling J_{i-h} , the temperature-dependence of the impurity-induced magnetic susceptibility as shown in Fig. 1, can also be quantitatively explained with a simplified model Hamiltonian. It was shown by Sørensen et al. [44] that the full exchange Hamiltonian $\mathcal{H}_e + \mathcal{H}_e^{i-h}$ of the doped Haldane system at low doping levels can be replaced by an effective Hamiltonian $\tilde{\mathcal{H}}$ for describing the low-energy excitations. Following this approach the

effective Hamiltonians can be in our case written in the following form in the limit of low cross-impurity exchange coupling \tilde{J}' and low impurity-host exchange J_{i-h}

$$\tilde{\mathcal{H}}_{\text{Mg}} = \alpha \tilde{J}' \mathbf{S}_l \cdot \mathbf{S}_r, \quad (11)$$

$$\tilde{\mathcal{H}}_{\text{Co}} = \alpha J_{i-h} (\mathbf{S}_l \cdot \mathbf{S}_i + \mathbf{S}_i \cdot \mathbf{S}_r) + \alpha \tilde{J}' \mathbf{S}_l \cdot \mathbf{S}_r, \quad (12)$$

where $\alpha = 1.064$ [44]. Operators \mathbf{S}_l , \mathbf{S}_r represent the $S = 1/2$ effective spins induced at sites “left” and “right” of a particular impurity site reflecting the nature of the valence-bond-solid ground state [2]. In the case of \tilde{J}' , $J_{i-h} < J$, bound in-gap states with exponentially decaying correlations are predicted [44].

Combining the effective exchange Hamiltonians given by Eqs. (11), (12) and the Zeeman Hamiltonian of the spins in the external magnetic field of 100 mT, the low-temperature dependence of the uniform static susceptibility can be forecasted. In the inset of Fig. 1 the calculated values of the expectation value of the S_z operator multiplied by the level of doping is shown. This quantity is detected in the dc magnetization measurements, however it reveals the same information as the static susceptibility $\chi_0 \propto (\langle S_z^2 \rangle - \langle S_z \rangle^2)/k_B T$ as long as the magnetization vs. magnetic field curves are linear. In the calculation the above-obtained parameters $\tilde{J}' = -2$ K and $J_{i-h} = 14$ K were taken into account. The agreement with the experiment is rather good, especially if we recall that the impurity-induced susceptibility is given by

$$\chi_i = \frac{x N_A g \mu_B \langle S_z \rangle}{2B} = 11 \text{ emu/mol} \cdot \frac{x}{2} \langle S_z \rangle. \quad (13)$$

Although the experiment nicely follows the theoretical predictions, it should be noted that close to the phase-transition temperature the static spin-correlations effect makes the simple model picture unsuited. Nevertheless, the puzzle of the size of the low-temperature spin susceptibility in Co- and Mg-doped $\text{PbNi}_2\text{V}_2\text{O}_8$ samples can be unambiguously unraveled. In the case of the vacancy doping, the ferromagnetic coupling between the liberated end-chain spins is responsible for the upturn in the magnetic susceptibility. Here, it should be stressed that the size of the coupling constant does not have any impact on the temperature dependence of the susceptibility. On the other hand, antiferromagnetic coupling in the case of the Co-doped sample is responsible for the substantial suppression of the susceptibility in comparison to the Mg-doped compound, as it shifts the weight of the in-gap states towards higher energies. An anisotropic exchange is expected in the case of the Co^{2+} ions, which further broadens the calculated peak in magnetic susceptibility.

At the end, a short comment on Cu-doping is given. It was shown experimentally that the susceptibility curves of Cu-doped $\text{PbNi}_2\text{V}_2\text{O}_8$ were virtually indistinguishable from curves corresponding to Mg-doped compounds above the phase-transition temperature when the doping level of Cu^{2+} ions was twice the doping level of Mg^{2+} ions [12]. This finding is in line with our results. Namely, the

antiferromagnetic exchange of Cu^{2+} impurities to Ni^{2+} spins is expected to have a high value, so that the low-energy excitations are solely given by the ferromagnetic coupling of the impurity-liberated spins. The ratio of the susceptibilities thus reflects the ratio of the effective spins $\tilde{S}_{\text{Mg}} = 1$ and $\tilde{S}_{\text{Cu}} = 1/2$.

V. CONCLUSIONS

In this paper an explanation of the low-temperature magnetic properties in magnetically and nonmagnetically doped Haldane compound $\text{PbNi}_2\text{V}_2\text{O}_8$ has been presented. The results of the dc magnetization and the electron spin resonance measurements were efficiently associated to provide an insight into the problem of the impurity-induced long-range magnetic ordering. The ESR approach revealed the strength of the ferromagnetic coupling between spin degrees of freedom liberated at both sites of the vacancies in the case of nonmagnetic Mg-doping, as well as the importance of the magnetic interactions between these delocalized spin clusters. On the

other hand, we were also able to evaluate the impurity-host exchange in compounds doped with magnetic Co^{2+} impurities through the bottleneck-type of the impurity-induced broadening of the ESR spectra. This coupling proved essential for the appearance of the in-gap magnetic excitations. It allowed a rather accurate prediction of the suppression of the low-temperature magnetic susceptibility in Co-doped compounds through a simplified effective exchange model. Additionally, the ESR measurements revealed information about the thermal vibrations in the investigated system through the determination of the Debye temperature.

Acknowledgments

We thank the General Secretariat for Science & Technology (Greece) and the former Ministry of Education, Science and Sport of the Republic of Slovenia for the financial support through a Greece-Slovenia "Joint Research & Technology Program".

-
- [1] F. D. M. Haldane, Phys. Rev. Lett., **50**, 1153, (1983).
 - [2] I. Affleck, T. Kennedy, E. H. Lieb and H. Tasaki, Phys. Rev. Lett., **59**, 799, (1987).
 - [3] M. Hagiwara, et al., Phys. Rev. Lett., **65**, 3181, (1990).
 - [4] E. W. Hudson, et al., Nature, **411**, 920, (2001).
 - [5] J. Villain, R. Bidaux, J. P. Carton and R. Conte, J. Phys. (Paris), **41**, 1263, (1980).
 - [6] M. Hase, et al., Phys. Rev. Lett., **71**, 4059, (1993).
 - [7] J. Lussier, S. M. Coad, D. F. McMorrow and D. McK Paul, J. Phys.: Condens. Matter, **7**, L325, (1995).
 - [8] T. Masuda, et al., Phys. Rev. Lett., **80**, 4566, (1998).
 - [9] P. E. Anderson, J. Z. Liu and R. N. Shelton, Phys. Rev. B, **56**, 11014, (1997).
 - [10] M. Azuma, et al., Phys. Rev. B, **55**, R8658, (1997).
 - [11] A. Oosawa, T. Ono and H. Tanaka, Phys. Rev. B, **66**, 020405(R), (2002).
 - [12] Y. Uchiyama, et al., Phys. Rev. Lett., **83**, 632, (1999).
 - [13] K. Uchinokura, T. Masuda, Y. Uchiyama and R. Kuroda, J. Magn. Magn. Mater., **226-230**, 431, (2001).
 - [14] S. Imai, T. Masuda, T. Matsuoka, and K. Uchinokura, arXiv:cond-mat/0402595 (2004, unpublished).
 - [15] K. Uchinokura, et al., Physica B, **284-288**, 1641, (2000).
 - [16] M. Laukamp, et al., Phys. Rev. B, **57**, 10755, (1998).
 - [17] A. Zorko, et al., Phys. Rev. B, **65**, 144449, (2002).
 - [18] D. Arčon, A. Zorko and A. Lappas, Europhys. Lett., **65**, 109, (2004).
 - [19] A. Zorko, D. Arčon, A. Lappas, Z. Jaglicic, to be published.
 - [20] A. Lappas, et al., Phys. Rev. B, **66**, 014428, (2002).
 - [21] I. Mastoraki, A. Lappas, R. Schneider and J. Giapintzakis, Appl. Phys. A Suppl., **74**, S640, (2002).
 - [22] I. Mastoraki, et al., J. Solid State Chem., **177**, 2404, (2004).
 - [23] I. Dzyaloshinsky, J. Phys. Chem. Solids, **4**, 241, (1958).
 - [24] T. Moriya, Phys. Rev., **120**, 91, (1960).
 - [25] A. Zorko, Ph.D. thesis, University of Ljubljana, 2004.
 - [26] Y. J. Kim, M. Greven, U. Wiese and R. J. Birgeneau, Eur. Phys. J. B, **4**, 291, (1998).
 - [27] T. Masuda, K. Uchinokura, T. Hayashi and N. Miura, Phys. Rev. B, **66**, 174416, (2002).
 - [28] A. Zheludev, et al., Phys. Rev. B, **62**, 8921, (2000).
 - [29] T. G. Castner and M. S. Seehra, Phys. Rev. B, **4**, 38, (1971).
 - [30] K. Nagata, T. Nishino, T. Hirokawa and T. Komatsubara, J. Phys. Soc. Jpn., **44**, 813, (1978).
 - [31] D. Hone and K. G. Petzinger, Phys. Rev. B, **6**, 245, (1972).
 - [32] P. M. Richards, in *Local Properties of Low-Dimensional Antiferromagnets*, edited by K. A. Müller (Nord Holland Publishing Company, Amsterdam, 1976), p. 539.
 - [33] P. M. Richards, Phys. Rev. B, **10**, 805, (1974).
 - [34] J. R. Pilbrow, *Transition Ion Electron Paramagnetic Resonance* (Oxford University Press, Oxford, 1990).
 - [35] J. E. Gulley and V. Jaccarino, Phys. Rev. B, **6**, 58, (1972).
 - [36] H. van der Vlist, A. F. M. Arts and H. W. de Wijn, Phys. Rev. B, **30**, 5000, (1984).
 - [37] A. Abragam, *Principles of Nuclear Magnetism* (Oxford University Press, Oxford, 1961).
 - [38] R. J. Radwanski and Z. Ropka, Physica B, **345**, 107, (2004).
 - [39] R. D. Hogg, S. V. Vernon and V. Jaccarino, Solid State Commun., **23**, 781, (1977).
 - [40] K. Białas-Borgiel, D. Skrzypek and E. Zipper, J. Phys. C: Solid St. Phys., **13**, 6251, (1980).
 - [41] H. Manaka and I. Yamada, Phys. Rev. B, **62**, 14279, (2000).
 - [42] A. Zheludev, T. Masuda, K. Uchinokura and S. E. Nagler, Phys. Rev. B, **64**, 134415, (2001).
 - [43] V. N. Glazkov, et al., JETP, **93**, 143, (2001).

- [44] E. S. Sørensen and I. Affleck, Phys. Rev. B, **51**, 16115, (1995).